IOPscience iopscience.iop.org

Home Search Collections Journals About Contact us My IOPscience

The electronic structure of point defects in semiconductor alloys: simplified approximations

This article has been downloaded from IOPscience. Please scroll down to see the full text article.

1992 J. Phys.: Condens. Matter 4 2209

(http://iopscience.iop.org/0953-8984/4/9/014)

View the table of contents for this issue, or go to the journal homepage for more

Download details:
IP Address: 171.66.16.159
The article was downloaded on 12/05/2010 at 11:25

Please note that terms and conditions apply.

J. Phys.: Condens. Matter 4 (1992) 2209–2216. Printed in the UK

The electronic structure of point defects in semiconductor alloys: simplified approximations

Amita Das and Vijay A Singh
Department of Physics, Indian Institute of Technology, Kanpur, Uttar Pradesh 208016, India

Received 20 March 1991, in final form 24 June 1991

Abstract. We present a simplified tight-binding-based coherent-potential approximation (CPA) formalism for the host electronic structure of semiconductor alloys (e.g. $Ga_{1-x}Al_xAs$). Several schemes to locate the gap level due to point defects are discussed. In particular, we introduce a novel scheme: the deep-level approximation. We also point out that the vacancy results in the CPA are identical with the simpler virtual-crystal approximation. We discuss our results by presenting numerical results in $Ga_{1-x}Al_xAs$ and $GaAs_{1-x}Sb_x$.

1. Introduction

Semiconductor alloys (e.g. $Ga_{1-x}Al_xAs$ and $GaAs_{1-x}Sb_x$) may be regarded as a substitutionally disordered system. The disordered alloy structure in which the occupancy of the anion or cation (or both) site is probablistic and can be replaced (using mean-field theories) by an effective ordered structure in which all the disordered sites are equivalent. This replacement is, however, at the cost of several physical characteristics of the original system. In the original disordered system there can be localization effects, which are largely washed out by the effective ordered crystal which replaces it.

A realistic description of a disordered medium could be achieved by very large cluster calculations averaged over all possible configurations. This method is computationally feasible only for very small cluster sizes, which probably do not do justice to real systems. In our work we have concentrated on the mean field and in particular on the coherent-potential approximation (CPA) description [1] of the disordered medium.

The presence of point defects in semiconductors may give rise to an energy level inside the forbidden band gap of the semiconductor. Technologically it becomes important that the defect which gives rise to the energy level should be identified so that measures could be taken to control its concentration in the semiconductor host. The gap level Z_d due to a defect with potential strength V can be identified with the help of the well known Koster–Slater (KS) equation [2].

We endeavour to incorporate the effect of disorder in the alloy structure self-consistently using an approximate form of the CPA theory developed by us. In section 2 we present the approximate form of the CPA for multiband realistic cases. We also attempt to put our formalism in perspective by discussing related work. In section 3 we show that, as far as the location of the energy level due to vacancies is concerned, both the CPA and the virtual-crystal approximation (VCA) give identical results. This suggests

0953-8984/92/092209 + 08 $04.50 © 1992 IOP Publishing Ltd

that a perturbation approach to an ultra-deep level in a semiconductor can be employed. We call it the deep-level approximation (DLA). Section 4 contains the conclusion.

2. Formalism

We shall illustrate in this section the method adopted by us to introduce a CPA description of the disordered host. We are dealing with substitutional and not positional disorder of the lattice. Hence, the underlying symmetry of the lattice remains the same as that of the tetrahedral group (T_d). The basis functions that we have chosen for our calculations decompose into four irreducible representations of the T_d group: two are of A_1 type (each of dimensionality one) and the remaining two are of the type T_2 (each of dimensionality three). A_1 is a totally symmetric representation which is invariant under all group transformations. We shall refer to it as an S state. The irreducible representation T_2 has the same transformation properties as the simple functions x, y and z under the T_d symmetry operations. The basis functions for this irreducible representation could be chosen as ψ_x, ψ_y and ψ_z which have an axial symmetry about $0X$, $0Y$ and $0Z$ Cartesian axes, respectively. We shall refer to them as P states.

The Hamiltonian expressed in the above symmetry-adapted basis will be separated into two blocks as follows:

$$\mathbf{H} = \begin{bmatrix} \mathbf{H}_{A_1} & 0 \\ 0 & \mathbf{H}_{T_2} \end{bmatrix}. \tag{2.1}$$

$\mathbf{H}_{A_1}$ is a matrix of size (2×2) corresponding to two A_1 representations. $\mathbf{H}_{T_2}$ corresponds to the two T_2 representations and is of size 6×6. The two representations of the A_1 as well as the T_2 have, as their basis, functions which are centred either at the anion or at the cation site. Furthermore, the Hamiltonian does not couple the basis functions of T_2, centred at the same site but having axial symmetry about a different axis. Thus $\mathbf{H}_{T_2}$ reduces to three (2×2) matrices corresponding to basis functions having symmetry about x, y and z axes, respectively. These three sets of matrices, however, are identical since the tetrahedral structure does not distinguish between the three axial directions.

A disordered Hamiltonian can be broken into a random part V and a configuration-independent part W. Thus

$$H = W + V. \tag{2.2}$$

The random part is assumed to be site diagonal hence

$$H = W + \sum_j V_j. \tag{2.3}$$

Here j represents the site index. We have chosen W to be our input VCA Hamiltonian, and we shall be incorporating the CPA corrections due to the random part $\Sigma_j V_j$ to this. The random potential can be written as

$$V_j = \sum_m |mR_j)(\varepsilon_j - \bar{\varepsilon})(mR_j|. \tag{2.4}$$

Here m standards for an S-like state and three P-like T_2 states. ε_j takes values ε_A or ε_B

depending on whether the atom A or B is occupying the site j. $\bar{\varepsilon}$ is the VCA energy which is given by

$$\bar{\varepsilon} = c_A \varepsilon_A + c_B \varepsilon_B. \tag{2.5}$$

Here c_A and c_B denote the concentration of A and B types of atom in the alloy.

The CPA formalism replaces the configuration-averaged one-electron Green function by an effective Green function

$$G_{\mathrm{eff}} = 1/(Z - H_{\mathrm{eff}}). \tag{2.6}$$

H_{eff} is defined as

$$H_{\mathrm{eff}} = W + \boldsymbol{\Sigma} \tag{2.7a}$$

$$H_{\mathrm{eff}} = W + \sum_j \boldsymbol{\Sigma}_j. \tag{2.7b}$$

$\boldsymbol{\Sigma}_j$ is termed the self-energy of the system and is obtained from the condition that the single-site scattering matrix $\mathbf{t}_j$ when averaged over all configurations is zero. $\boldsymbol{\Sigma}$ can be viewed as a block diagonal matrix; each block is identified by a particular site j and is of size (8×8) for the above-mentioned eight states. Furthermore, the translational symmetry of the averaged crystal ensures that each block is identical. Thus Bloch's theorem can be invoked and $\boldsymbol{\Sigma}$ can be represented in a reduced Bloch space of size (8×8). The tetrahedral symmetry further decomposes $\boldsymbol{\Sigma}$ into two blocks of A_1 and T_2 representations. We write $\boldsymbol{\Sigma}$ as

$$\boldsymbol{\Sigma} = \begin{bmatrix} \boldsymbol{\Sigma}_{A_1} & 0 \\ 0 & \boldsymbol{\Sigma}_{T_2} \end{bmatrix}$$

$$\boldsymbol{\Sigma}_{A_1} = \begin{bmatrix} \boldsymbol{\Sigma}^{a}_{A_1} & 0 \\ 0 & \boldsymbol{\Sigma}^{c}_{A_1} \end{bmatrix}$$

where the superscripts a and c stand for anion and cation, respectively.

$$\boldsymbol{\Sigma}_{T_2} = \begin{bmatrix} \boldsymbol{\Sigma}_{T_{2x}} & & \mathbf{0} \\ & \boldsymbol{\Sigma}_{T_{2y}} & \\ \mathbf{0} & & \boldsymbol{\Sigma}_{T_{2z}} \end{bmatrix}.$$

Each of the $\boldsymbol{\Sigma}_{T_{2x}}$, $\boldsymbol{\Sigma}_{T_{2y}}$, $\boldsymbol{\Sigma}_{T_{2z}}$ can be further decomposed into cation and anion subspaces as has been shown for $\boldsymbol{\Sigma}_{A_1}$. The off-diagonal elements of $\boldsymbol{\Sigma}$ have been neglected, which is in agreement with the approximation invoked by Chen and Sher [3].

Symmetry about the x, y and z axes further ensures that

$$\boldsymbol{\Sigma}_{T_{2x}} = \boldsymbol{\Sigma}_{T_{2y}} = \boldsymbol{\Sigma}_{T_{2z}} = \boldsymbol{\Sigma}_{T_2}.$$

The CPA equation for this multiband case is a matrix equation of the form

$$\bar{\boldsymbol{\Sigma}}(z) = -[\bar{\boldsymbol{\varepsilon}}_A - \bar{\boldsymbol{\Sigma}}(z)]\, \bar{\mathbf{F}}(z)\, [\bar{\boldsymbol{\varepsilon}}_B - \bar{\boldsymbol{\Sigma}}(z)]. \tag{2.8}$$

The above-mentioned symmetry reduces it to a set of four coupled scalar equations

$$\bar{\Sigma}_{r,d}(z) = -[\boldsymbol{\varepsilon}_{A_{r,d}} - \bar{\Sigma}_{r,d}(z)]\bar{F}_{r,d}(z)[\bar{\boldsymbol{\varepsilon}}_{B_{r,d}} - \bar{\Sigma}_{r,d}(z)]. \tag{2.9}$$

Here the subscript r refers to the symmetry and the subscript d to the cation or anion subspaces. These equations are coupled via the Green function. An approximate method

of decoupling the above equations can be devised using the partitioning technique of Löwdin [4].

The component Green function $F_{\mathrm{r,d}}$ can be evaluated from the component density of states by the following equation:

$$F_{\mathrm{r,d}} = \frac{1}{N} \int \frac{\mathrm{d}\varepsilon\, \rho_{\mathrm{r,d}}(\varepsilon)}{z - \Sigma_{\mathrm{r,d}} - \varepsilon}. \qquad (2.10)$$

Using equations (2.9) and (2.10) the CPA corrections to the Green function can be determined.

Perhaps it is worthwhile to put our proposed form of the CPA for alloy semiconductors into perspective. An early work on this subject is by Sen and Cohen [5] who applied it to a model two-(s)band semiconductor. Stroud and Ehrenreich [6] applied a CPA formalism using pseudopotentials to calculate the electronic structure of Si–Ge alloys. Chen and Sher [7] employed a bond-orbital-model-based CPA to calculate the valence bands of several semiconductor alloys. They concluded that the CPA should replace earlier theories such as the VCA since the band-gap bowing parameter is significantly influenced by alloy disorder. In another pioneering effort, Spicer *et al* [8] demonstrated the feasibility of the CPA by making detailed comparison with experiment for the alloy $Hg_{1-x}Cd_xTe$. They employed atomic orbitals reconstructed from empirical pseudopotentials. Subsequently the present authors together with Krishnamurthy [9] employed a similar methodology to Si–Ge alloys. Besides one-electron properties such as the density of states they investigated the electron drift mobility. Myles and co-workers [10] developed a tight-binding CPA formalism and applied it to semiconductor alloys. A tight-binding-based molecular CPA (MCPA) formalism was proposed by Hass *et al* [11]. A perturbational method for impurity level splitting based on Roth's [12] effective-medium approximation (EMA) was proposed by Hasbun and Roth [13] for impurities in $GaAs_xP_{1-x}$. The importance of local environment effects on a point defect in semiconductor alloys was also emphasized by Mariette *et al* [14]. They proposed a single CPA methodology for individual bands α ($\alpha \equiv \Gamma$, X_1 and L). Our approach employs the Vogl *et al* [15] ten-band tight-binding parameters and is similar to that of Myles and co-workers [10]. It differs in detail from [10] and has a simplified structure.

Next we consider the problem of point defects in alloys. Point defects could be either substitutional impurities or vacancies present in the disordered alloy semiconductors.

The defect potential caused by the substitution of an impurity atom for a host atom has the following three distinct contributions:

(i) a short-range central cell potential;
(ii) a long-range Coulomb potential;
(iii) an electron–lattice interaction caused by the lattice relaxation around the impurity.

We shall ignore the screened Coulomb potential and assume a simple realistic model in which there is no lattice relaxation. We shall deal essentially with the central cell potential which is the difference between the atomic potentials of the impurity and the host atom.

The single-site defect can be identified with V_j in equation (2.3). In this case the index j corresponds to a particular site and is not a running index over all sites.

Thus the defect potential can be made block diagonal in this symmetry-adapted basis; it contains one (2×2) a_1 symmetry matrix and three (2×2) t_2 symmetry matrices.

The three (2 × 2) P-type symmetry matrices will be identical. The defect potential is then

$$\mathbf{V}^{\Gamma}_{i,j} = \begin{bmatrix} \varepsilon^{\Gamma}_{c,imp} - \varepsilon^{\Gamma}_{c,host} & V^{\Gamma}_{imp} - V^{\Gamma}_{host} \\ V^{\Gamma}_{imp} - V^{\Gamma}_{host} & \varepsilon^{\Gamma}_{a,imp} - \varepsilon^{\Gamma}_{a,host} \end{bmatrix}.$$

Γ represents the symmetry and i and j ≡ {c, a} correspond to the cation and anion, respectively.

We approximate the atomic energy difference between two atoms in a solid to be similar to the difference between free atoms. We also neglect the off-diagonal elements as they scale as the inverse square of the bond length and we have accounted for these in our VCA Hamiltonian W. Thus, if the impurity is at the cation site, then

$$\mathbf{V}^{\Gamma}_{i,j} = \begin{bmatrix} \varepsilon^{\Gamma}_{c,imp} - \varepsilon^{\Gamma}_{c,host} & 0 \\ 0 & 0 \end{bmatrix}.$$

The bound-state energy E_b can be obtained by the solution of the following K–S-type equation:

$$1/V_{\Gamma,d} = F_{\Gamma,d}. \tag{2.11}$$

3. The deep-level approximation for defects

If the defect level is a simple vacancy on a cation or an anion sublattice, then the corresponding defect potential is infinity. From equation (2.11) we see that the defect level due to vacancy will then be given by the zeros of $F_{\Gamma,d}$. Here Γ denotes the symmetry of the level and d the sublattice which has a vacancy as a defect.

Substituting the value of $F_{\Gamma,d}$ in equation (2.9) we get the value of $\Sigma_{\Gamma,d}$, which is zero. One thus observes that for the vacancy level the CPA result is identical with the VCA result. This suggests that a perturbation approach to an ultra-deep level in alloy semiconductor can be employed. This is the DLA which is obtained from the self-consistent CPA equation by retaining first-order terms in the inverse defect potential $1/V$.

The self-consistent CPA equation is (dropping the subscripts for lattice and symmetry)

$$\Sigma(z_d) = -[\varepsilon_A - \Sigma(z_d)]F(z_d)[\varepsilon_B - \Sigma(z_d)]. \tag{3.1}$$

Using the K–S equation,

$$F(z_d) = 1/V = \delta \tag{3.2}$$

where δ is a small parameter. Thus

$$\Sigma(z_d) = -[\varepsilon_A - \Sigma(z_d)]\delta[\varepsilon_B - \Sigma(z_d)]. \tag{3.3}$$

Retaining first-order terms in δ, one gets

$$\Sigma(z_d) = -\delta\varepsilon_A\varepsilon_B. \tag{3.4}$$

Moreover

$$F(z_d) = F_{VCA}(z') \tag{3.5}$$

where

$$z_d = z' - \Sigma(z_d)$$

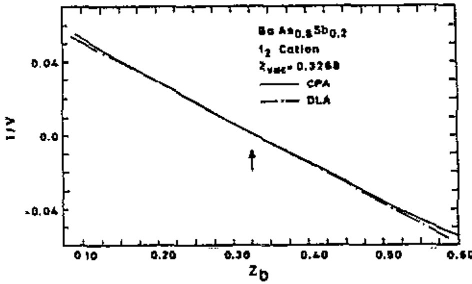

Figure 1. A plot of the inverse defect potential strength versus the t_2 cation defect level in the fundamental gap of $GaAs_{0.8}Sb_{0.2}$: ——, results obtained by using the CPA; —·—·, results obtained by using the DLA. Note that the vacancy level shown by an arrow is predicted at 0.33 eV by both the theories.

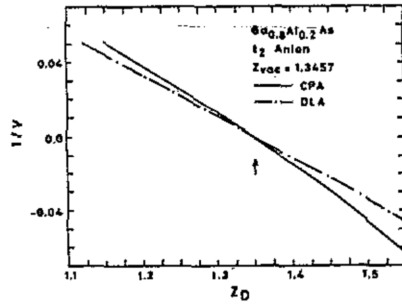

Figure 2. A plot of the inverse defect potential strength versus the t_2 anion defect level in the fundamental gap of $Ga_{0.8}Al_{0.2}As$: ——, results obtained by using the CPA; —·—·, results obtained by using the DLA. Note that the vacancy level shown by an arrow is predicted at 1.35 eV by both the theories.

or

$$z_d = z' + \delta\varepsilon_A\varepsilon_B. \tag{3.6}$$

Let z_c be the location of the defect level for the vacancy. Expanding $F_{VCA}(z')$ about $F_{VCA}(z_c)$, one gets, on neglecting higher powers,

$$F_{VCA}(z') = F_{VCA}(z_c) + (z' - z_c)F'_{VCA}(z_c). \tag{3.7}$$

We have chosen δ to be sufficiently small; hence z' can be assumed to be quite close to z_c. However, $F_{VCA}(z_c) = 0$, since z_c is by definition a vacancy level and the VCA result is exact for it. Hence

$$\delta = (z' - z_c)F'_{VCA}(z_c). \tag{3.8}$$

From equations (3.13) and (3.14),

$$z_d = z_c + \delta/F'_{VCA}(z_c) + \delta\varepsilon_A\varepsilon_B. \tag{3.9}$$

Thus knowing the vacancy level and the slope of the VCA Green function at the vacancy level the deep defect level for a given defect potential can be directly read from equation (3.9).

Figure 1 depicts the t_2 cation defect level in the fundamental gap of $GaAs_{0.8}Sb_{0.2}$. The cation vacancy level for this system is at 0.33 eV above the valence band edge. The agreement between the DLA and the CPA is excellent near z_{vac}.

Figure 2 depicts a similar comparison between the DLA and the CPA for the t_2 anion defect level in the fundamental gap of $Ga_{0.8}Al_{0.2}As$. The DLA results deviate from the CPA results as we move away from the vacancy level which is at $z_{vac} = 1.35$ eV. Figure 3 shows a t_2 cation level in $Ga_{0.6}Al_{0.4}As$.

As demonstrated earlier, the VCA and CPA give identical results for the vacancy level in an alloy semiconductor. It is worthwhile exploring the differences between the two for a general gap level. It must be noted that, when the host energies for the two species are close to each other, then the VCA ought to be satisfactory (small-scattering regime). Let us consider the case of $GaAs_{0.8}Sb_{0.2}$. From the parameters given by Vogl *et al* [15] we observe that the cation p-orbital energy $E(p, c)$ for GaAs and GaSb differ only by

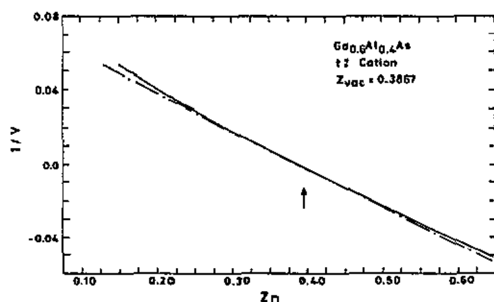

Figure 3. A plot of the inverse defect potential strength versus the t_2 cation defect level in the fundamental gap of $Ga_{0.8}Al_{0.4}As$: ——, results obtained by using the CPA; —·—·, results obtained by using the DLA. Note that the vacancy level shown by an arrow is predicted at 0.39 eV by both the theories.

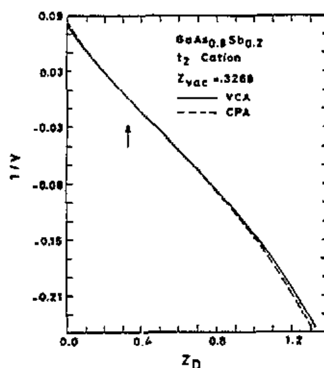

Figure 4. A plot of defect potential strength versus the t_2 cation defect level in $GaAs_{0.8}Sb_{0.2}$ as given by the CPA (——) and the VCA (– – –). The common vacancy level predicted by the theories is shown by an arrow at 0.327 eV.

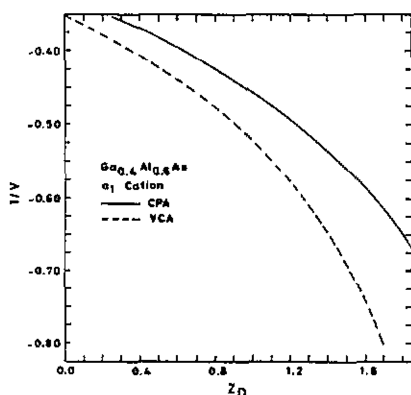

Figure 5. A plot of defect potential strength versus the a_1 cation defect level in $Ga_{0.4}Al_{0.8}As$ as given by the CPA (——) and the VCA (– – –). Note that there is no vacancy level within the fundamental gap.

20%. Thus in figure 4 the defect level as given by the CPA is almost indistinguishable from that given by the VCA.

When the energy difference between the two species is large, we expect the CPA and the VCA to differ considerably. This is borne out by the plot in figure 5 in which the a_1 cation defect is given for $Ga_{1-x}Al_xAs$. The energy $E(s, c)$ differs for two systems GaAs and AlAs, in this case by 56%.

4. Conclusion

We have presented simple mean-field approximations to account for the effect of disorder on the electronic structure of point defects in semiconductor alloys. The work can be extended in several directions, formal and otherwise. Formally, one may employ the Hellmann–Feynman theorem to calculate the total energy of and the forces on point defects. This work could then address issues, such as metastability, which are important

for the DX centre [16, 17]. It would also be desirable to include charge consistency in the sense of the local-density approximation. This would, however, destroy the inherent simplicity of our approach. It is perhaps worthwhile to think of our approach as a methodology for quick and reliable estimates.

Acknowledgment

This work was supported in part by a grant on the 'Calculation of the Electronic Structure of Disordered Alloys' from the Department of Science and Technology, Government of India.

References

[1] Soven P 1967 *Phys. Rev.* **156** 809
Taylor D 1967 *Phys. Rev.* **156** 1017
[2] Koster G F and Slater J C 1954 *Phys. Rev.* **95** 1167
[3] Chen A B and Sher A 1978 *Phys. Rev.* B **17** 4726
[4] Löwdin P O 1962 *J. Appl. Phys.* suppl 1 **33** 251
[5] Sen P and Cohen M H 1972 *J. Non-Cryst. Solids* **8–10** 147
[6] Stroud D and Ehrenreich H 1970 *Phys. Rev.* B **2** 3197
[7] Chen A B and Sher A 1978 *Phys. Rev. Lett.* **40** 900; 1979 *Phys. Rev.* B **19** 3057; 1981 *Phys. Rev.* B **23** 5360
[8] Spicer W E, Silberman J A, Morgan J, Lindau I, Wilson J A, Chen A B and Sher A 1982 *Phys. Rev. Lett.* **49** 948
[9] Krishnamurthy S, Sher A and Chen A B 1986 *Phys. Rev.* B **33** 1026
[10] Gregg J R, Myles C W and Shen Y T 1987 *Phys. Rev.* B **35** 2532
[11] Hass K C, Lempert R J and Ehrenreich H 1984 *Phys. Rev. Lett.* **52** 77
Hass K C, Ehrenreich H and Velicky B 1983 *Phys. Rev.* B **27** 1088
The latter is a single-site CPA calculation for $Hg_{1-x}Cd_xTe$.
[12] Roth L M 1974 *Phys. Rev.* B **9** 2476
[13] Hasbun J and Roth L M 1989 *J. Appl. Phys.* **65** 4801
[14] Mariette H, Chevallier J and Leroux Hugen P 1980 *Phys. Rev.* B **21** 5706
[15] Vogl P, Hjalmarson H P and Dow J D 1983 *J. Phys. Chem. Solids* **44** 365
[16] Lang D V 1986 *Deep Centers in Semiconductors* ed S T Pantelides (New York: Gordon and Breach) pp 489–539
[17] Lang D V and Logan R A 1977 *Phys. Rev. Lett.* **39** 635–9
Logan D V and Jaros M 1979 *Phys. Rev.* B **19** 1015–30